Title	Conferring robustness to path-planning for image-based control
Author(s)	Chesi, G; Shen, T
Citation	IEEE Transactions on Control Systems Technology, 2012, v. 20 n. 4, p. 950-959
Issued Date	2012
URL	http://hdl.handle.net/10722/155764
Rights	©2012 IEEE. Personal use of this material is permitted. However, permission to reprint/republish this material for advertising or promotional purposes or for creating new collective works for resale or redistribution to servers or lists, or to reuse any copyrighted component of this work in other works must be obtained from the IEEE.

Conferring Robustness to Path-Planning for Image-Based Control

Graziano Chesi, *Senior Member, IEEE*, and Tiantian Shen, *Student Member, IEEE*

***Abstract*—Path-planning has been proposed in visual servoing for reaching the desired location while fulfilling various constraints. Unfortunately, the real trajectory can be significantly different from the reference trajectory due to the presence of uncertainties on the model used, with the consequence that some constraints may not be fulfilled hence leading to a failure of the visual servoing task. This paper proposes a new strategy for addressing this problem, where the idea consists of conferring robustness to the path-planning scheme by considering families of admissible models. In order to obtain these families, uncertainty in the form of random variables is introduced on the available image points and intrinsic parameters. Two families are considered, one by generating a given number of admissible models corresponding to extreme values of the uncertainty, and one by estimating the extreme values of the components of the admissible models. Each model of these families identifies a reference trajectory, which is parametrized by design variables that are common to all the models. The design variables are hence determined by imposing that all the reference trajectories fulfill the required constraints. Discussions on the convergence and robustness of the proposed strategy are provided, in particular showing that the satisfaction of the visibility and workspace constraints for the second family ensures the satisfaction of these constraints for all models bounded by this family. The proposed strategy is illustrated through simulations and experiments.**

***Index Terms*—Eye-in-hand, path-planning, robustness, uncertainty, visual servoing.**

I. Introduction

VISUAL servoing consists of automatically positioning a robot end-point via closed-loop control by using visual information, typically the view of a camera mounted on the robot end-point. The control law has to ensure that the camera reaches a desired location which is identified by the image projections of some object features. Various control laws have been proposed to address this task, starting from the pioneering image-based visual servoing (IBVS), position-based visual servoing (PBVS), and 2 1/2 D visual servoing. See for instance [1]–[3].

Path-planning has been introduced in order to fulfill physical constraints and optimize a desired performance. Typically this strategy determines a reference trajectory that the camera attempts to follow by using a trajectory tracker. This has been proposed in several ways, e.g., by exploiting repulsive potential fields [4], [5], screw-motion trajectories [6], interpolation of the collineation matrix [7], homography-based partial pose estimation [8], helicoidal paths [9], modulation of the control gains [10], polynomial parametrizations [11], and search trees in camera and joint spaces [12].

Unfortunately, the real trajectory followed by the camera can be significantly different from the reference trajectory due to the presence of uncertainties on the model used in the planning phase. As a consequence, by using existing path-planning schemes it may happen that the real trajectory does not optimize the considered performance, and even worse, does not fulfill some of the required constraints hence leading to a failure of the visual servoing task. The reader is referred to [13]–[15] for effects of uncertainties on visual servoing.

This paper proposes a new strategy for conferring robustness to path-planning for image-based control. The idea consists of considering families of admissible models rather than a model only in the planning phase. In order to obtain these families, uncertainty in the form of random variables is introduced on the available image points and intrinsic parameters. Two families are considered, one by generating a given number of admissible models corresponding to extreme values of the uncertainty, and one by estimating the extreme values of the components of the admissible models. Each model of these families identifies a reference trajectory, which is parametrized by using polynomials in the trajectory abscissa and by introducing design variables that are common to all models. The design variables are hence determined by imposing that all the reference trajectories fulfill the required constraints and guarantee a worst-case cost of the considered performance. Once the reference trajectory is computed, its image projection is tracked by using image-based control. Discussions on the convergence and robustness of the proposed strategy are hence provided, in particular showing that the satisfaction of the visibility and workspace constraints for the models in the second family ensures the satisfaction of these constraints for all models bounded by this family. Simulations and experiments illustrate the proposed strategy. A preliminary version of this paper appeared in [16].

This paper is organized as follows. Section II introduces the notation and some preliminaries. Section III describes the modeling of the uncertainty and the parametrization of the trajectory. Section IV explains the estimation of the admissible models and the computation of the trajectory. Section V illustrates the proposed approach through some examples. Last, Section VI concludes this paper with some final remarks.

Manuscript received December 21, 2010; accepted May 03, 2011. Manuscript received in final form May 16, 2011. Date of publication June 23, 2011; date of current version May 22, 2012. Recommended by Associate Editor L. Villani. This work was supported in part by Grant HKU711208E.

The authors are with the Department of Electrical and Electronic Engineering, University of Hong Kong, Hong Kong (e-mail: chesi@eee.hku.hk; tiantianshen@gmail.com).

Color versions of one or more of the figures in this paper are available online at http://ieeexplore.ieee.org.

Digital Object Identifier 10.1109/TCST.2011.2157346

II. Preliminaries

The notation is as follows: w.r.t.: with respect to; $\mathbb{R}$: real number set; $SO(3)$: set of rotation matrices in $\mathbb{R}^{3\times 3}$; $\mathbf{0}$: null vector/matrix (size specified by the context); $\mathbf{1}$: vector/matrix with all entries equal to 1 (size specified by the context); $\mathbf{I}$: identity matrix (size specified by the context); $\mathbf{e}_i$: ith column of the identity matrix (size specified by the context); $\mathbf{X}^T$: transpose of vector/matrix $\mathbf{X}$; $||\mathbf{X}||$: 2-norm of vector/matrix $\mathbf{X}$; $||\mathbf{X}||_\infty$: infinity norm of vector/matrix $\mathbf{X}$; $[\mathbf{x}]_\times$: skew-symmetric matrix of vector $\mathbf{x} \in \mathbb{R}^3$, i.e.,

$$[\mathbf{x}]_\times = \begin{pmatrix} 0 & -x_3 & x_2 \\ x_3 & 0 & -x_1 \\ -x_2 & x_1 & 0 \end{pmatrix}.$$

Let $F^\# = (\mathbf{O}^\#, \mathbf{c}^\#)$ and $F^* = (\mathbf{O}^*, \mathbf{c}^*)$ denote two camera frames expressed w.r.t. an absolute frame F^{abs}, where $\mathbf{O}^\#$, $\mathbf{O}^* \in SO(3)$ define the orientations and $\mathbf{c}^\#$, $\mathbf{c}^* \in \mathbb{R}^3$ define the origins of $F^\#$ and F^*. Let $\mathbf{q}_1, \ldots, \mathbf{q}_N \in \mathbb{R}^3$ be 3-D points expressed w.r.t. F^{abs}. Assuming the case of projective camera models, we have that $\mathbf{q}_i$ projects onto the image planes of $F^\#$ and F^* at the points $\mathbf{p}_i^\# = \left(p_{i,1}^\#, p_{i,2}^\#, 1\right)^T$ and $\mathbf{p}_i^* = \left(p_{i,1}^*, p_{i,2}^*, 1\right)^T$ defined by

$$d_i^\# \mathbf{p}_i^\# = \mathbf{A}\mathbf{O}^{\#T}\left(\mathbf{q}_i - \mathbf{c}^\#\right) \quad d_i^* \mathbf{p}_i^* = \mathbf{A}\mathbf{O}^{*T}\left(\mathbf{q}_i - \mathbf{c}^*\right) \quad (1)$$

where $d_i^\#$, $d_i^* \in \mathbb{R}$ are the depths of the points w.r.t. $F^\#$ and F^*, and $\mathbf{A} \in \mathbb{R}^{3\times 3}$ is the upper-triangular matrix containing the camera intrinsic parameters. We then define

$$\mathbf{p}^\# = \left(p_{1,1}^\#, p_{1,2}^\#, \ldots, p_{N,1}^\#, p_{N,2}^\#\right)^T$$
$$\mathbf{p}^* = \left(p_{1,1}^*, p_{1,2}^*, \ldots, p_{N,1}^*, p_{N,2}^*\right)^T. \quad (2)$$

The visual servoing task is as follows. The camera is positioned at F^* and the image projections of $\mathbf{q}_1, \ldots, \mathbf{q}_N$ are recorded in $\mathbf{p}^*$. Then, the camera is moved to another location, denoted by $F^\#$, and the image projections of the same points are recorded in $\mathbf{p}^\#$. The task consists of steering the camera from $F^\#$ to F^* by exploiting $\mathbf{p}^\#$, $\mathbf{p}^*$. This task is performed in closed-loop, and $\mathbf{p}^\#$ is progressively replaced by the vector of image features seen from the current location of the camera.

Path-planning methods have been developed for addressing constraints satisfaction and performance optimization in visual servoing. These methods typically determine a reference trajectory that the camera attempts to follow by exploiting image-based control. This reference trajectory is computed on the basis of the available model, which consists of the estimates $\hat{\mathbf{p}}^\#$, $\hat{\mathbf{p}}^*$, $\hat{\mathbf{A}}$ of the quantities $\mathbf{p}^\#$, $\mathbf{p}^*$, $\mathbf{A}$.

III. Uncertainty Modeling and Trajectory Parametrization

A. Uncertainty Modeling

Our idea is to plan a reference trajectory in the image that satisfies the required constraints and optimizes the considered performance for a family of admissible estimates $\hat{\mathbf{p}}^\#$, $\hat{\mathbf{p}}^*$, $\hat{\mathbf{A}}$. This family can be generated by introducing uncertainties on $\mathbf{p}^\#$, $\mathbf{p}^*$, $\mathbf{A}$. Here we consider the specific case of uniform additive uncertainties for clarity of presentation (this case is also one of those typically used for modeling uncertainties), but one can consider also different cases. Let us express $\hat{\mathbf{p}}^\#$ and $\hat{\mathbf{p}}^*$ as

$$\hat{\mathbf{p}}^\# = \mathbf{p}^\# + \mathbf{n}^\# \qquad \hat{\mathbf{p}}^* = \mathbf{p}^* + \mathbf{n}^* \quad (3)$$

where $\mathbf{n}^\#$, $\mathbf{n}^* \in \mathbb{R}^{2n}$ are random variables representing the image noise. It is assumed that these random variables are bounded according to

$$||\mathbf{n}^\#||_\infty \leq \eta \qquad ||\mathbf{n}^*||_\infty \leq \eta \quad (4)$$

where $\eta \in \mathbb{R}$ depends on the intensity of the image noise. Similarly, we express $\hat{\mathbf{A}}$ as

$$\hat{\mathbf{A}} = \mathbf{A} + \mathbf{\Lambda}$$
$$\mathbf{A} = \begin{pmatrix} A_1 & A_2 & A_3 \\ 0 & A_4 & A_5 \\ 0 & 0 & 1 \end{pmatrix}$$
$$\mathbf{\Lambda} = \begin{pmatrix} \lambda_1 & \lambda_2 & \lambda_3 \\ 0 & \lambda_4 & \lambda_5 \\ 0 & 0 & 0 \end{pmatrix} \quad (5)$$

where $A_1, \ldots, A_5 \in \mathbb{R}$ are the intrinsic parameters and $\lambda_1, \ldots, \lambda_5 \in \mathbb{R}$ are random variables satisfying, for some bounds $\lambda_1^-, \lambda_1^+, \ldots, \lambda_5^-, \lambda_5^+ \in \mathbb{R}$

$$\lambda_i \in \left[\lambda_i^-, \lambda_i^+\right]. \quad (6)$$

The difficulty we have to face is that different values of the uncertainties $\mathbf{n}^\#$, $\mathbf{n}^*$, $\mathbf{\Lambda}$ lead to different estimates of the camera pose between $F^\#$ and F^*, and hence to different reference trajectories. In order to address this problem, we parametrize each possible reference trajectory through an admissible estimate of the camera pose and through design variables that are common to all the reference trajectories as explained in the sequel.

B. Trajectory Parametrization

In order to simplify the description, let us suppose without loss of generality that $F^\#$ coincides with F^{abs}, hence implying that $\mathbf{O}^\# = \mathbf{I}$ and $\mathbf{c}^\# = \mathbf{0}$. Let us parametrize the reference trajectory from $F^\#$ to a generic location with frame $(\mathbf{R}, \mathbf{t})$ expressed w.r.t. F^{abs}, where $\mathbf{R} \in SO(3)$ and $\mathbf{t} \in \mathbb{R}^3$. We denote the camera frame along the reference trajectory as $F(w, \mathbf{R}, \mathbf{t})$, where $w \in [0, 1]$ is the trajectory abscissa, with $w = 0$ and $w = 1$ indicating the initial and the desired locations. We hence have

$$F(0, \mathbf{R}, \mathbf{t}) = (\mathbf{I}, \mathbf{0}) \qquad F(1, \mathbf{R}, \mathbf{t}) = (\mathbf{R}, \mathbf{t}). \quad (7)$$

The camera frame $F(w, \mathbf{R}, \mathbf{t})$ is expressed as

$$F(w, \mathbf{R}, \mathbf{t}) = (\mathbf{O}(w, \mathbf{R}), \mathbf{c}(w, \mathbf{t})) \quad (8)$$

where the functions $\mathbf{O}(w, \mathbf{R}) \in SO(3)$ and $\mathbf{c}(w, \mathbf{t}) \in \mathbb{R}^3$ define the orientation and the origin which depend on w, $\mathbf{R}$, $\mathbf{t}$. From (7), these functions satisfy

$$\mathbf{O}(0, \mathbf{R}) = \mathbf{I},\ \mathbf{c}(0, \mathbf{t}) = \mathbf{0}$$
$$\mathbf{O}(1, \mathbf{R}) = \mathbf{R},\ \mathbf{c}(1, \mathbf{t}) = \mathbf{t}. \quad (9)$$

We express $\mathbf{O}(w,\mathbf{R})$ via quaternion, and hence write

$$\mathbf{O}(w,\mathbf{R}) = \frac{\mathbf{\Omega}(\mathbf{b}(w,\mathbf{R}))}{\|\mathbf{b}(w,\mathbf{R})\|^2} \tag{10}$$

where $\mathbf{b}(w,\mathbf{R}) \in \mathbb{R}^4$ is a nonzero vector and $\mathbf{\Omega}(\cdot)$ is given by

$$\mathbf{\Omega}(\mathbf{b}) = \begin{pmatrix} b_1^2-b_2^2-b_3^2+b_4^2 & 2(b_1b_2-b_3b_4) & 2(b_1b_3+b_2b_4) \\ 2(b_1b_2+b_3b_4) & -b_1^2+b_2^2-b_3^2+b_4^2 & 2(b_2b_3-b_1b_4) \\ 2(b_1b_3-b_2b_4) & 2(b_2b_3+b_1b_4) & -b_1^2-b_2^2+b_3^2+b_4^2 \end{pmatrix}. \tag{11}$$

Indeed, $\mathbf{\Omega}(\mathbf{b}(w,\mathbf{R})) \in SO(3)$ for any $\mathbf{b}(w,\mathbf{R}) \neq \mathbf{0}$. Moreover, for any $\mathbf{O}(w,\mathbf{R}) \in SO(3)$, there exists $\mathbf{b}(w,\mathbf{R}) \neq \mathbf{0}$ satisfying (10). See, e.g., [15], [17], [18] for uses of quaternion. We indicate such a vector as $\mathbf{b}(w,\mathbf{R}) = \boldsymbol{\xi}(\mathbf{O}(w,\mathbf{R}))$, where $\boldsymbol{\xi}(\cdot)$ is a suitable function. From (9) it follows that $\mathbf{b}(w,\mathbf{R})$ satisfies:

$$\mathbf{b}(0,\mathbf{R}) = (0,0,0,1)^T \qquad \mathbf{b}(1,\mathbf{R}) = \boldsymbol{\xi}(\mathbf{R}). \tag{12}$$

Next, we parameterize the functions $\mathbf{O}(w,\mathbf{R})$ and $\mathbf{c}(w,\mathbf{t})$ via polynomials. In particular, we use polynomials of degree δ_B and δ_C for $\mathbf{b}(w,\mathbf{R})$ and $\mathbf{c}(w,\mathbf{t})$, respectively

$$\begin{aligned} \mathbf{b}(w,\mathbf{R}) &= \tilde{\mathbf{B}}\left(w^{\delta_B}, w^{\delta_B-1}, \ldots, w, 1\right)^T \\ \mathbf{c}(w,\mathbf{t}) &= \tilde{\mathbf{C}}\left(w^{\delta_C}, w^{\delta_C-1}, \ldots, w, 1\right)^T \end{aligned} \tag{13}$$

where $\tilde{\mathbf{B}} \in \mathbb{R}^{4\times\delta_B+1}$ and $\tilde{\mathbf{C}} \in \mathbb{R}^{3\times\delta_C+1}$. The conditions (9) are satisfied if and only if

$$\tilde{\mathbf{B}} = (\boldsymbol{\xi}(\mathbf{R}) - \mathbf{B}\cdot\mathbf{1} - \mathbf{e}_4, \mathbf{B}, \mathbf{e}_4) \qquad \tilde{\mathbf{C}} = (\mathbf{t} - \mathbf{C}\cdot\mathbf{1}, \mathbf{C}, \mathbf{0}) \tag{14}$$

where $\mathbf{B} \in \mathbb{R}^{4\times\delta_s-1}$ and $\mathbf{C} \in \mathbb{R}^{3\times\delta_C-1}$ are free matrices. Therefore, the camera frame $F(w,\mathbf{R},\mathbf{t})$ along the reference trajectory is parameterized by the trajectory abscissa w, the desired location with frame $(\mathbf{R},\mathbf{t})$, and the matrices $\mathbf{B}$ and $\mathbf{C}$.

IV. Admissible Models, Trajectory Computation, and Visual Servoing

A. Estimating Admissible Models

Given the true values of $\mathbf{p}^\#$, $\mathbf{p}^*$, $\mathbf{A}$, the camera pose between $F^\#$ and F^* can be recovered in the case of non-coplanar features with $N \geq 8$ through the essential matrix algorithm or through the homography matrix algorithm relative to a virtual plane. If the features are known to be coplanar with $N \geq 4$, the camera pose can be computed through the homography matrix algorithm. See for instance [17], [19], [20] and references therein. These procedures provide a normalized translational component if no additional information is available but $\mathbf{p}^\#$, $\mathbf{p}^*$, $\mathbf{A}$ because, in such a case, the translation can be computed only up to a scale factor which stands for the unknown distance between the origins of $F^\#$ and F^*. We indicate the estimate returned by any of these algorithms as

$$E_R(\mathbf{p}^\#,\mathbf{p}^*,\mathbf{A}) \in SO(3) \qquad E_t(\mathbf{p}^\#,\mathbf{p}^*,\mathbf{A}) \in \mathbb{R}^3. \tag{15}$$

However, $\mathbf{p}^\#$, $\mathbf{p}^*$, $\mathbf{A}$ are unknown, and according to (3)–(6) one has a family of admissible camera poses corresponding to triplets $\mathbf{p}^\#$, $\mathbf{p}^*$, $\mathbf{A}$ in the set

$$\mathcal{I} = \{(\mathbf{p}^\#,\mathbf{p}^*,\mathbf{A})\text{: (3) and (5) hold for some } (\mathbf{n}^\#,\mathbf{n}^*,\mathbf{\Lambda}) \in \mathcal{U}\} \tag{16}$$

where $\mathcal{U}$ is the set of admissible triplets $\mathbf{n}$, $\mathbf{n}^*$, $\mathbf{\Lambda}$ given by

$$\mathcal{U} = \left\{(\mathbf{n}^\#,\mathbf{n}^*,\mathbf{\Lambda}) : n_i^\#, n_i^* \in [-\eta,\eta], \lambda_i \in \left[\lambda_i^-, \lambda_i^+\right]\right\}. \tag{17}$$

Let us denote with $\mathcal{V}$ the set of vertices of $\mathcal{U}$, i.e.,

$$\mathcal{V} = \left\{(\mathbf{n}^\#,\mathbf{n}^*,\mathbf{\Lambda}) : n_i^\#, n_i^* \in \{-\eta,\eta\},\ \lambda_i \in \{\lambda_i^-, \lambda_i^+\}\right\}. \tag{18}$$

Let $v_1,\ldots,v_M$ be a set of triplets in $\mathcal{V}$, and let us denote the ith triplet v_i as $v_i = \left(\mathbf{n}_i^\#, \mathbf{n}_i^*, \mathbf{\Lambda}_i\right)$. Then, we define the camera pose $(\mathbf{R}_i,\mathbf{t}_i)$ associated with v_i as

$$\begin{aligned} \mathbf{R}_i &= E_R\left(\hat{\mathbf{p}}^\# - \mathbf{n}_i^\#, \hat{\mathbf{p}}^* - \mathbf{n}_i^*, \hat{\mathbf{A}} - \mathbf{\Lambda}_i\right) \\ \mathbf{t}_i &= E_t\left(\hat{\mathbf{p}}^\# - \mathbf{n}_i^\#, \hat{\mathbf{p}}^* - \mathbf{n}_i^*, \hat{\mathbf{A}} - \mathbf{\Lambda}_i\right). \end{aligned} \tag{19}$$

The camera poses $(\mathbf{R}_1,\mathbf{t}_1),\ldots,(\mathbf{R}_M,\mathbf{t}_M)$ are a family of admissible models which has been obtained by considering extreme values of the uncertainties on the image points and intrinsic parameters.

In addition, we introduce a reconstruction of the scene points $\mathbf{q}_1,\ldots,\mathbf{q}_N$ associated with the camera pose $(\mathbf{R}_i,\mathbf{t}_i)$, which we denote as

$$\mathcal{Q}_i = E_q\left(\hat{\mathbf{p}}^\# - \mathbf{n}_i^\#, \hat{\mathbf{p}}^* - \mathbf{n}_i^*, \hat{\mathbf{A}} - \mathbf{\Lambda}_i\right). \tag{20}$$

Each of the N reconstructions in the set $\mathcal{Q}_i$ can be found by solving a triangulation problem with 2 views, which amounts to determining the SVD of a 4×4 matrix whenever the standard algebraic criterion is adopted (see for instance [21] and references therein for triangulation with different criteria). Such reconstructions are normalized if the translations $\mathbf{t}_1,\ldots,\mathbf{t}_M$ are computed only up to a scale factor.

Hence, we define the estimated family of admissible models as

$$\mathcal{M}_1 = \left\{(\mathbf{R}_i,\mathbf{t}_i,\mathcal{Q}_i,\hat{\mathbf{A}} - \mathbf{\Lambda}_i),\ i = 1,\ldots,M\right\}. \tag{21}$$

B. Estimating Extreme Admissible Models

A problem with the family $\mathcal{M}_1$ introduced in Section IV-A is that it may not contain the extreme admissible models, i.e., the admissible models with extreme values of the model components. However, let us observe that computing such models is not trivial, as one should:

- repeat the computation of the camera pose and object reconstruction for all the triplets $\mathbf{p}^\#$, $\mathbf{p}^*$, $\mathbf{A}$ in the set $\mathcal{I}$, i.e., an infinite number of times;
- or attempt to solve several nonconvex optimization problems where the decision variables are the components of the uncertainty and the cost functions are the model components.

Another problem with the family $\mathcal{M}_1$ is that ensuring the satisfaction of the physical constraints for all the models in this family does not ensure the satisfaction of these constraints for all models bounded by this family (i.e., for the "intermediate" models) given its generic structure.

In order to cope with these problems while requiring a reasonable computational effort, we build a special family of estimates of the extreme admissible models starting from the family $\mathcal{M}_1$. Specifically, the idea is to determine the extreme values for each component of the camera pose and object reconstruction in the set of admissible models. In particular, let us define the extreme values for the rotation matrix as

$$\begin{aligned} r_{j,k,-} &= \min_{i=1,\dots,M} (j,k)\text{th entry of } \mathbf{R}_i \\ r_{j,k,+} &= \max_{i=1,\dots,M} (j,k)\text{th entry of } \mathbf{R}_i \end{aligned} \tag{22}$$

where $j,k=1,2,3$. Similarly, we introduce the extreme values for the translation vector as

$$\begin{aligned} t_{j,-} &= \min_{i=1,\dots,M} j\text{th entry of } \mathbf{t}_i \\ t_{j,+} &= \max_{i=1,\dots,M} j\text{th entry of } \mathbf{t}_i \end{aligned} \tag{23}$$

and for the set of object reconstructions as

$$\begin{aligned} q_{j,-} &= \min_{\mathbf{q}\in\mathcal{Q}_i,\ i=1,\dots,M} j\text{th entry of } \mathbf{q} \\ q_{j,+} &= \max_{\mathbf{q}\in\mathcal{Q}_i,\ i=1,\dots,M} j\text{th entry of } \mathbf{q} \end{aligned} \tag{24}$$

where $j=1,2,3$. Hence, we estimate the extreme values for the model components via

$$\mathcal{W}_R = \left\{\mathbf{R}\in\mathbb{R}^{3\times 3}\text{: its } (j,k)\text{th entry lies in } [r_{j,k,-}, r_{j,k,+}]\right\} \tag{25}$$

for the rotation

$$\mathcal{W}_t = \left\{\mathbf{t}\in\mathbb{R}^3 : \text{its } j\text{th entry lies in } [t_{j,-}, t_{j,+}]\right\} \tag{26}$$

for the translation, and

$$\mathcal{W}_q = \left\{\mathbf{q}\in\mathbb{R}^3 : \text{its } j\text{th entry lies in } [q_{j,-}, q_{j,+}]\right\} \tag{27}$$

for the object reconstruction.

The sought family of model estimates is hence given by

$$\begin{aligned} \mathcal{M}_2 = \big\{&(\mathbf{R},\mathbf{t},\mathbf{q},\hat{\mathbf{A}}-\mathbf{\Lambda}) : \\ &\mathbf{R}\in\mathcal{W}_R,\ \mathbf{t}\in\mathcal{W}_t,\ \mathbf{q}\in\mathcal{W}_q,\ \lambda_i\in\left\{\lambda_i^-,\lambda_i^+\right\}\big\}. \end{aligned} \tag{28}$$

Before proceeding it is worth making some observations about the family $\mathcal{M}_2$. First, the models of this family correspond to the vertices of a hyperrectangle in the space of $\mathbf{R}$, $\mathbf{t}$, $\mathbf{q}$, $\mathbf{A}$. This will allow us to derive robustness properties for the planned path as it will be explained in Section IV-D.

Second, the family $\mathcal{M}_2$ contains also matrices $\mathbf{R}$ that are not rotation matrices. This conservatism is the cost to pay for obtaining a simple estimate of the set of admissible rotation matrices. An alternative can be to set the (j,k)th entry of the rotation matrices in $\mathcal{M}_2$ equal to a constant value if the range for such an entry is smaller than a chosen threshold. Also, one can define the set $\mathcal{M}_2$ by using only one rotation matrix (in particular the one given by the estimates $\hat{\mathbf{p}}^{\#}$, $\hat{\mathbf{p}}^{*}$, $\hat{\mathbf{A}}$) in order to avoid to include non-rotation matrices.

Another observation concerns the matrices of the intrinsic parameters in $\mathcal{M}_2$. In fact, since these matrices will be used in the computation of the trajectory only for imposing the visibility constraint, one can equivalently redefine $\mathcal{M}_2$ by keeping only the matrices of the intrinsic parameters with the largest focal lengths. Indeed, since it is reasonable to suppose that the principal point in these matrices lies inside the image, then one has that the visibility constraint is satisfied for all admissible focal lengths whenever it is satisfied for their maximum values.

C. Trajectory Computation

For clarity of description, let us denote with $(\mathbf{R},\mathbf{t})$ a generic estimate of the camera pose, and with $\mathbf{q}_j$ a generic estimate of the jth scene point (in the sequel we will replace these generic quantities with the estimates previously obtained).

The visibility constraint along the camera trajectory can be expressed as

$$\mathbf{e}_k^T\mathbf{p}_j(w,\mathbf{R},\mathbf{t})\in[\sigma_{k,1},\sigma_{k,2}]\ \forall\, k=1,2$$

where $\mathbf{p}_j(w,\mathbf{R},\mathbf{t})$ is the projection of $\mathbf{q}_j$ onto $F(w,\mathbf{R},\mathbf{t})$, and $\sigma_{1,1},\sigma_{1,2},\dots\in\mathbb{R}$ are the screen limits. We have that

$$\begin{aligned} \mathbf{p}_j(w,\mathbf{R},\mathbf{t}) &= \left(\frac{f_{j,1}(w,\mathbf{R},\mathbf{t})}{f_{j,3}(w,\mathbf{R},\mathbf{t})}, \frac{f_{j,2}(w,\mathbf{R},\mathbf{t})}{f_{j,3}(w,\mathbf{R},\mathbf{t})}, 1\right)^T \\ f_{j,k}(w,\mathbf{R},\mathbf{t}) &= \mathbf{e}_k^T\mathbf{A}\mathbf{\Omega}(\mathbf{b}(w,\mathbf{R}))^T(\mathbf{q}_j(w,\mathbf{R},\mathbf{t})-\mathbf{c}(w,\mathbf{t})). \end{aligned} \tag{29}$$

Hence, the visibility constraint is fulfilled whenever $s(w)\geq 0$ for all $s(w)\in\mathcal{S}^{\text{vis}}$, where $\mathcal{S}^{\text{vis}}$ is the set of polynomials

$$\begin{aligned} \mathcal{S}^{\text{vis}} = \big\{&s(w) = (-1)^l(\sigma_{k,l}f_{j,3}(w,\mathbf{R},\mathbf{t}) - f_{j,k}(w,\mathbf{R},\mathbf{t})), \\ &j=1,\dots,N,\ k=1,2,\ l=1,2\big\}. \end{aligned} \tag{30}$$

Let us consider now the workspace constraint. This constraint imposes that the camera origin remains in an allowed region of the scene, that we describe w.r.t. F^* as

$$G = \left\{\mathbf{x}\in\mathbb{R}^3 : g_j(\mathbf{x})\geq 0,\ j=1,\dots,N_g\right\} \tag{31}$$

where $g_1,g_2,\dots : \mathbb{R}^3\to\mathbb{R}$ are polynomials. Clearly, this description cannot easily handle complicated workspace representations such as occupancy grids, nevertheless one can enlarge the variety of considerable workspace representations by increasing the degree and the number of polynomials $g_j(\mathbf{x})$. Since the origin of $F(w,\mathbf{R},\mathbf{t})$ w.r.t. F^* is given by $\mathbf{\Omega}(\mathbf{b}(w,\mathbf{R}))^T(\mathbf{c}(w,\mathbf{t})-\mathbf{t})$, the workspace constraint is fulfilled if and only if $s(w)\geq 0$ for all $s(w)\in\mathcal{S}^{\text{wor}}$, where

$$\begin{aligned} \mathcal{S}^{\text{wor}} = \big\{&s(w) = g_j(\mathbf{\Omega}(\mathbf{b}(w,\mathbf{R}))^T(\mathbf{c}(w,\mathbf{t})-\mathbf{t})), \\ &j=1,\dots,N_g\big\}. \end{aligned} \tag{32}$$

Last, let us consider the joint constraint (also known as kinematic constraint), and let $h_j(\mathbf{O},\mathbf{c})$ be the j-th joint depending

on the location of the end-point $(\mathbf{O}, \mathbf{c})$. This function has to satisfy

$$h_j(\mathbf{O}, \mathbf{c}) \in [\tau_{j,1}, \tau_{j,2}] \tag{33}$$

for all locations $(\mathbf{O}, \mathbf{c})$ along the camera trajectory and for all $j = 1, \ldots, N_h$, where $\tau_{j,1}$ and $\tau_{j,2}$ are the limits for the jth joint and N_h is the number of joints. This is equivalent to impose that $s(w) \geq 0$ for all $s(w) \in \mathcal{S}^{\text{joi}}$, where

$$\mathcal{S}^{\text{joi}} = \big\{ s(w) = (-1)^l (\tau_{j,l} - h_j(\boldsymbol{\Omega}(\mathbf{b}(w, \mathbf{R})), \mathbf{c}(w, \mathbf{t}))), \\ j = 1, \ldots, N_h,\ l = 1, 2 \big\}. \tag{34}$$

In the case that the function $h_j(\boldsymbol{\Omega}(\mathbf{b}(w, \mathbf{R})), \mathbf{c}(w, \mathbf{t}))$ is non-polynomial, one can replace it with a truncated Taylor expansion, whose approximation error can be reduced by increasing the degree of the expansion. Then, in the case that the inverse kinematic $h_j(\mathbf{O}, \mathbf{c})$ is not available, one can obtain the trajectory of the joints from the trajectory of the camera pose through integration as proposed in [4].

A reference trajectory that satisfies the required constraints and optimizes a cost of interest φ (e.g., visibility margin, trajectory length, etc.) is obtained as

$$\begin{aligned} &\min_{\mathbf{B},\mathbf{C}} \varphi \\ &\text{subject to } s(w) \geq 0 \; \forall \, w \in [0, 1], \\ &\quad \forall \, s(\cdot) \in \mathcal{S}, \; \forall \, (\mathbf{R}, \mathbf{t}, \mathbf{q}, \mathbf{A}) \in \mathcal{M} \end{aligned} \tag{35}$$

where $\mathcal{S}$ is the total set of constraints given by

$$\mathcal{S} = \mathcal{S}^{\text{vis}} \cup \mathcal{S}^{\text{wor}} \cup \mathcal{S}^{\text{joi}} \tag{36}$$

and $\mathcal{M}$ is the set of admissible models considered, either $\mathcal{M}_1$ defined in Section IV-A, or $\mathcal{M}_2$ defined in Section IV-B. The polynomials in $\mathcal{S}$ typically do not have an explicit representation, but they can be constructed through simple algorithms from the problem data according to the definitions (29)–(34). In Section IV-D we will discuss the solution of problem (35). Before proceeding it is useful making the following observations.

First, the use of polynomials in the proposed strategy is motivated by the fact that polynomials can approximate arbitrarily well continuous functions on bounded domains, which is reasonably the case of visual servoing, and by the fact that establishing the positivity of some functions as required in (35) is easier if such functions are polynomial rather than transcendental.

Second, similarly to visibility, workspace, and joint constraints, one can consider also occlusion constraints in the planning phase. Specifically, this can be done by imposing that the camera does not enter certain regions of the scene (i.e., through an additional workspace constraint) or by imposing that the image features along the trajectory do not get too close to certain image areas (corresponding to objects between the camera and the reference points). Details on these extensions are omitted for conciseness.

D. Trajectory Tracking, Convergence and Robustness

Problem (35) can be solved in several ways, for instance by adopting standard nonlinear optimization tools such as the simplex algorithm or modified[1] Newton's algorithm. When using such tools, the satisfaction of the constraints at each iteration can be simply decided by computing the roots of univariate polynomials thanks to the introduced parametrization of the trajectory. Let us observe that convergence to a minimizer $(\mathbf{B}, \mathbf{C})$ is typically guaranteed by the tools previously mentioned. Clearly, this minimizer is in general only local, i.e., it is possible that the found minimizer is not global: let us observe, however, that this is not necessarily a problem, in the sense that any local minimizer ensures satisfaction of the constraints, and the difference with a global minimizer consists of providing a sub-optimal value of the cost function (which is reasonably less important than satisfying the constraints). Also, polynomial constraints such as those in the optimization problem (35) can be handled via LMI optimizations, see for instance [11] and the recent survey [22], which have the advantage to be free of local-only minimizers (details are omitted for conciseness).

After solving (35), one builds the trajectory of the image features determined by the found pair $(\mathbf{B}, \mathbf{C})$. Specifically, the trajectory of the j-th image point is given by $\mathbf{p}_j(w, \hat{\mathbf{R}}, \hat{\mathbf{t}})$ where $(\hat{\mathbf{R}}, \hat{\mathbf{t}})$ is the camera pose corresponding to the available estimates, i.e.,

$$\hat{\mathbf{R}} = E_R(\hat{\mathbf{p}}^{\#}, \hat{\mathbf{p}}^{*}, \hat{\mathbf{A}}) \qquad \hat{\mathbf{t}} = E_t(\hat{\mathbf{p}}^{\#}, \hat{\mathbf{p}}^{*}, \hat{\mathbf{A}}). \tag{37}$$

An image-based trajectory tracker is then used to follow this trajectory following the idea introduced in [4]. Indeed, let us gather the image points $\mathbf{p}_j(w, \mathbf{R}_0, \mathbf{t}_0)$ into a vector $\mathbf{s}(w)$, and let $\mathbf{s}$ be a similar vector built with the image points in the current camera frame. The computed trajectory can be tracked via the control law

$$\mathbf{v} = \mathbf{L}^{+}(-\lambda_1(\mathbf{s} - \mathbf{s}(w)) + \dot{\mathbf{s}}(w)) \qquad w = 1 - e^{-\lambda_2 t} \tag{38}$$

where $\mathbf{v} \in \mathbb{R}^6$ is the camera velocity, $\mathbf{L}^{+}$ is the pseudoinverse of the interaction matrix between $\mathbf{s}$ and $\mathbf{v}$, and λ_1, $\lambda_2 \in \mathbb{R}$ are any positive scalars. Observe that $\dot{\mathbf{s}}(w)$ can be easily computed analytically since $\mathbf{s}(w)$ is parametrized via polynomials, and that the expression of w ensures exponential convergence of the trajectory abscissa to its final value (other expressions can be chosen). See also [23] about visual tracking.

Let us consider the convergence properties of the camera under the tracking law (38). We have that the camera converges to the desired location with the same convergence properties of IBVS. In fact, $\mathbf{v}$ in (38) can be expressed as

$$\mathbf{v} = \mathbf{v}_{\text{IBVS}} + \mathbf{o} \tag{39}$$

where $\mathbf{v}_{\text{IBVS}}$ is the standard IBVS control law, which is given by

$$\mathbf{v}_{\text{IBVS}} = -\lambda_1 \mathbf{L}^{+}(\mathbf{s} - \mathbf{s}^{*}) \tag{40}$$

[1]In order to ensure positive definiteness of the Hessian matrix and decrease of the cost function.

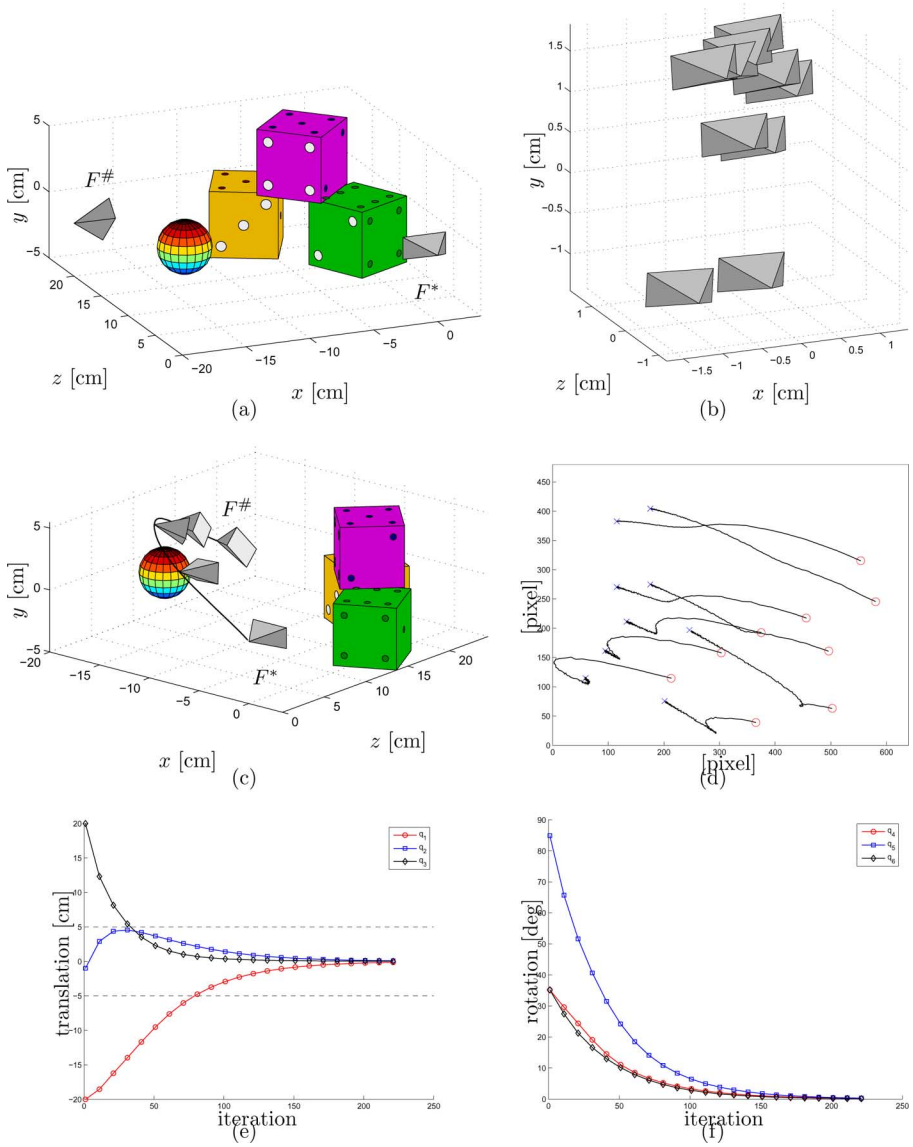

Fig. 1. Example 1. (a) Problem definition. (b) Some admissible desired locations. (c) 3D path obtained by tracking the planned path. (d) Camera view ("O": initial view; "X": desired view). (e) Translation evolution (dashed line: limit for joint q_2). (f) Rotation evolution.

and $\mathbf{o}$ is the remaining part of $\mathbf{v}$ which satisfies

$$\lim_{t\to\infty} ||\mathbf{o}|| = 0. \tag{41}$$

Indeed, as t increases, the trajectory abscissa w approaches 1, i.e., the desired location, and $||\dot{\mathbf{s}}(w)||$ approaches 0 since w converges to a finite value and $\mathbf{s}(w)$ is continuously differentiable.

Last, let us consider the robustness of the proposed strategy. As previously mentioned, considering the set of admissible models $\mathcal{M}_1$ in the optimization problem (35) provides some robustness to the planned trajectory in the sense that the satisfaction of the constraints are ensured for any quadruplet $(\mathbf{R}, \mathbf{t}, \mathbf{q}, \mathbf{A})$ in this set, while existing strategies ensures the satisfaction of the constraints only for the nominal model $(\hat{\mathbf{R}}, \hat{\mathbf{t}}, \hat{\mathcal{Q}}, \hat{\mathbf{A}})$. However, nothing can be said in general about the satisfaction of the constraints for the admissible models not considered in $\mathcal{M}_1$. Instead, as previously announced, the set of admissible models $\mathcal{M}_2$ allows one to say something more about this point. Indeed, if the visibility and workspace constraints of the optimization problem (35) are satisfied for the models in $\mathcal{M}_2$, then they are also satisfied for all intermediate models bounded by those in $\mathcal{M}_2$, i.e., for all models in the set

$$\bar{\mathcal{M}}_2 = \text{conv}\{(\mathbf{R}, \mathbf{t}, \mathbf{q}, \mathbf{A}) \in \mathcal{M}_2\} \tag{42}$$

where conv denotes the convex hull. In other words, the set $\bar{\mathcal{M}}_2$ contains all models where the entries of $\mathbf{R}$, $\mathbf{t}$, $\mathbf{q}$, $\mathbf{A}$ are allowed to vary within the extremes present in $\mathcal{M}_2$. This result is due to two reasons. First, the visibility and workspace constraints are multilinear functions of the quantities $\mathbf{R}$, $\mathbf{t}$, $\mathbf{q}$, $\mathbf{A}$, i.e., they are linear functions of any of these quantities whenever the others are fixed. Second, the set $\bar{\mathcal{M}}_2$ is an hyperrectangle in the space of $\mathbf{R}$, $\mathbf{t}$, $\mathbf{q}$, $\mathbf{A}$, and a multilinear function is positive in a hyperrectangle whenever it is positive at its vertices, which holds for the models in $\mathcal{M}_2$. Let us observe that this conclusion cannot be obtained for the joint constraint in general since it is not described by a multilinear function, but typically by a more complicated one.

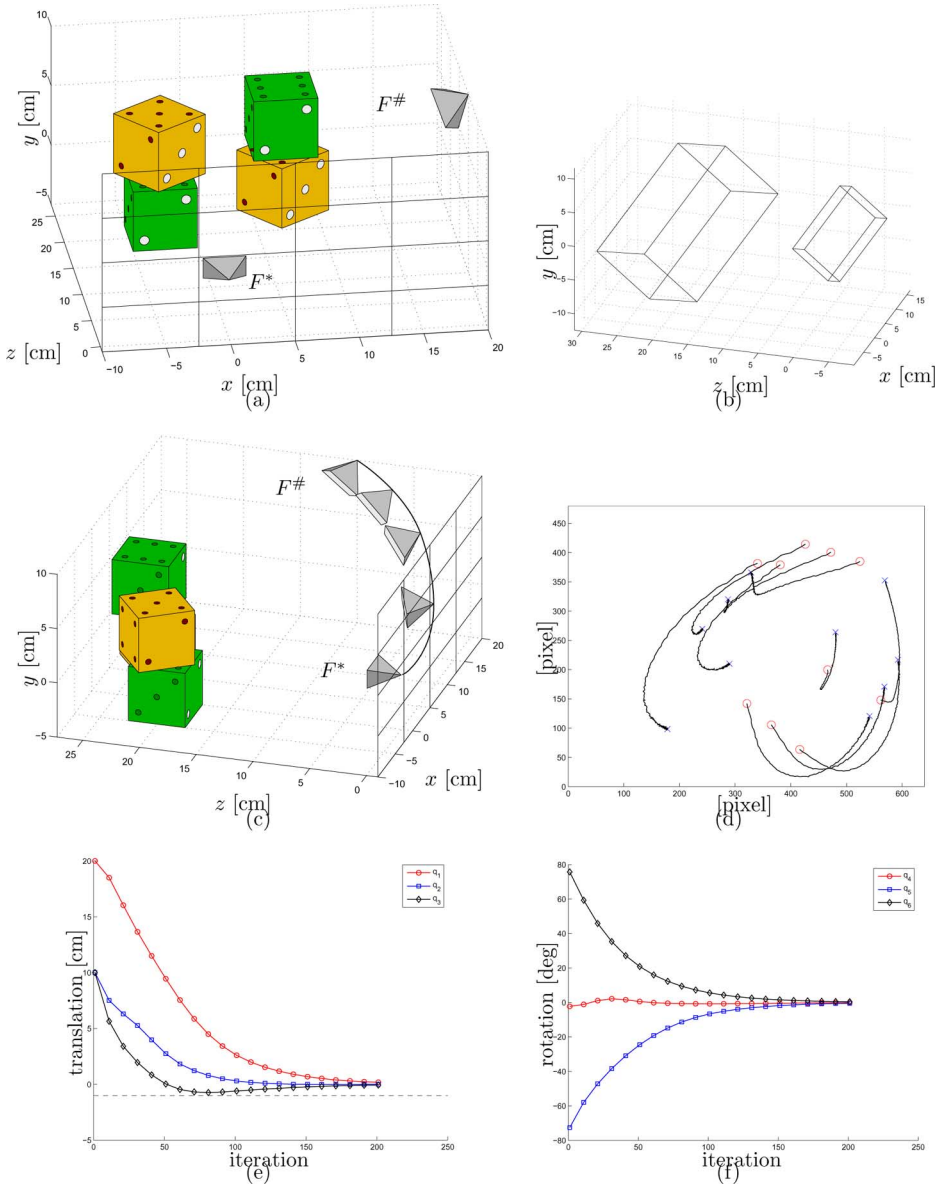

Fig. 2. Example 2. (a) Problem definition. (b) Worst-case positions for camera center and object points. (c) 3-D path obtained by tracking the planned path. (d) Camera view ("O": initial view; "X": desired view). (e) Translation evolution (dashed line: limit for joint q_3). (f) Rotation evolution.

V. Examples

In this section we present some illustrative examples of the proposed strategy. The trajectory tracker (38) is implemented by using the current value of the interaction matrix (computed with an estimate of the point depths at the desired location). This choice may allow to follow the planned trajectory more closely than by using a constant interaction matrix, though this latter solution requires less computations.

A. Simulation Results: Example 1

Let us consider the situation in Fig. 1(a) where the camera observes 9 large dots of three dices. The problem is to reach F^* from $F^\#$ while avoiding collisions with and occlusions due to the sphere, and keeping the joints within their limit (we consider the constraint $q_2 \in [-5, 5]$ cm, where q_2 represents the vertical coordinate of the camera). The relative position of the obstacle with respect to the desired location is supposed known. The CAD model of the object is unknown.

In order to reproduce conditions typical of real experiments, we add image noise to each entry of each image feature through random variables with uniform distribution in $[-1, 1]$ pixels, intrinsic calibration errors by choosing $\mathbf{A}$ and its estimate $\hat{\mathbf{A}}$ as

$$\mathbf{A} = \begin{pmatrix} 600 & 0 & 320 \\ 0 & 600 & 240 \\ 0 & 0 & 1 \end{pmatrix}, \quad \hat{\mathbf{A}} = \begin{pmatrix} 581 & 0 & 332 \\ 0 & 620 & 229 \\ 0 & 0 & 1 \end{pmatrix}$$

and extrinsic calibration errors by choosing the camera-robot transformation $(\mathbf{R}_E, \mathbf{t}_E)$ and its estimate $(\hat{\mathbf{R}}_E, \hat{\mathbf{t}}_E)$ as

$$\mathbf{R}_E = \mathbf{I},\ \mathbf{t}_E = \mathbf{0},\ \hat{\mathbf{R}}_E = e^{[(5,7.5,-10)^T \pi/180]_\times}$$
$$\hat{\mathbf{t}}_E = (-2, 1.5, 1)^T \text{ cm}.$$

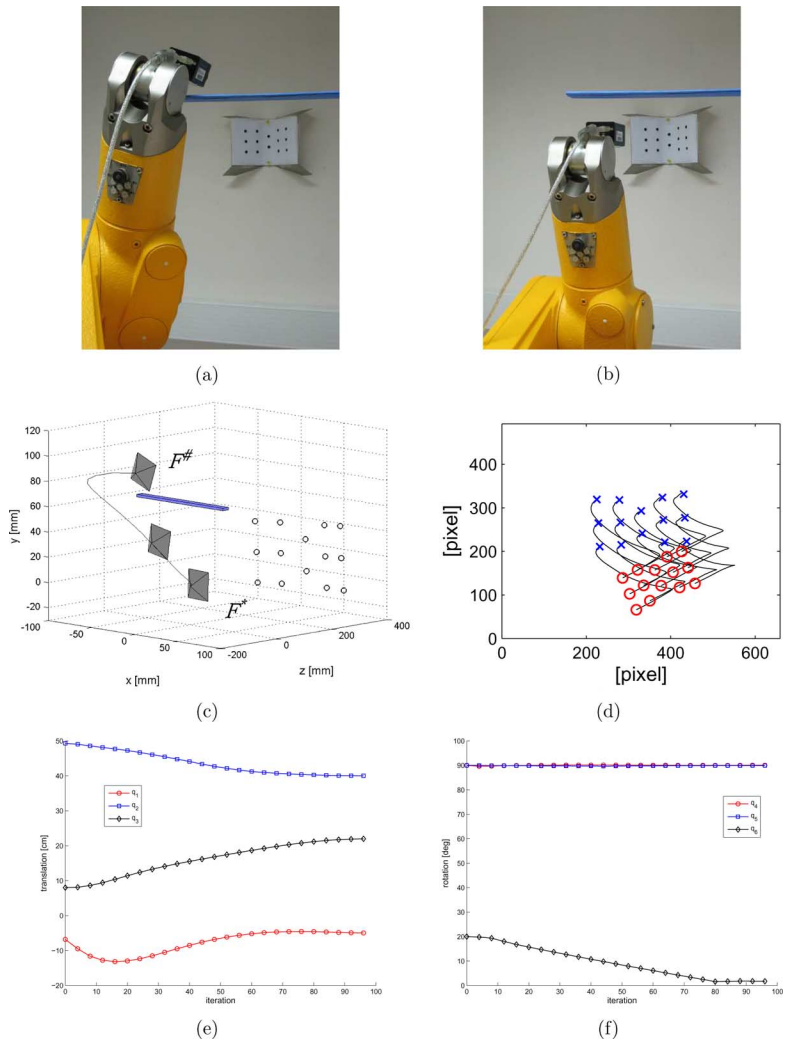

Fig. 3. Example 3. (a) Initial view. (b) Desired view. (c) 3-D path. (d) Camera view ("O": initial view; "X": desired view). (e) Translation evolution. (f) Rotation evolution.

Let us use the proposed approach for planning a robust reference trajectory. We introduce the uncertain model (3)–(5) with

$$\eta = 1 \text{ pixel},\ \lambda_i^- = 0.95\hat{A}_i,\ \lambda_i^+ = 1.05\hat{A}_i$$

hence considering uncertainty up to ± 1 pixel on each component of the image features, and up to $\pm 5\%$ on each intrinsic parameter of the camera.

The next step is to estimate the admissible camera poses. We consider the family of admissible models $\mathcal{M}_1$ that we obtain by selecting $M = 10$ and computing the camera poses $(\mathbf{R}_i, \mathbf{t}_i)$ in (19) through the essential matrix algorithm. Fig. 1(b) shows some admissible desired locations provided by these camera poses. Hence, we solve the robust path-planning problem (35) for $\delta_B = \delta_C = 2$ minimizing the trajectory length via the simplex algorithm, and from the found matrices $\mathbf{B}$ and $\mathbf{C}$ we determine the trajectory in the image domain, which is tracked by using the trajectory tracker (38). Fig. 1(c)–(f) show the obtained results.

For comparison, we attempt to solve the same problem with our previous approach in [11], where only one camera pose is considered: it follows that the final trajectory followed by the camera does not fulfill the joint constraint (the maximum value of q_2 is 5.61 cm). For completeness, we also consider the classic PBVS and IBVS: with PBVS all the points leave the field of view, while with IBVS the joint constraint is not fulfilled (the maximum value of q_2 is 8.62 cm).

B. Simulation Results: Example 2

Here we consider the situation shown in Fig. 2(a) where the problem is to reach F^* avoiding collisions with the vertical plane indicated by the grid, which may represent either a joint constraint or a workspace constraint (the plane equation is $q_3 = -1$, where q_3 represents the z-coordinate of the camera).

We introduce the uncertain model (3)–(5) as done in Example 1, and we consider this time the family of admissible models $\mathcal{M}_2$ obtained by selecting $M = 10$. Fig. 2(b) shows the estimated uncertain regions for the translation (represented by the camera center) and the object points, i.e., the hyperrectangles $\mathcal{W}_t$ and $\mathcal{W}_q$ (which are defined in the frame of the initial camera). Fig. 2(c)–(f) show the obtained results by solving the robust path-planning problem (35). As shown by the obtained

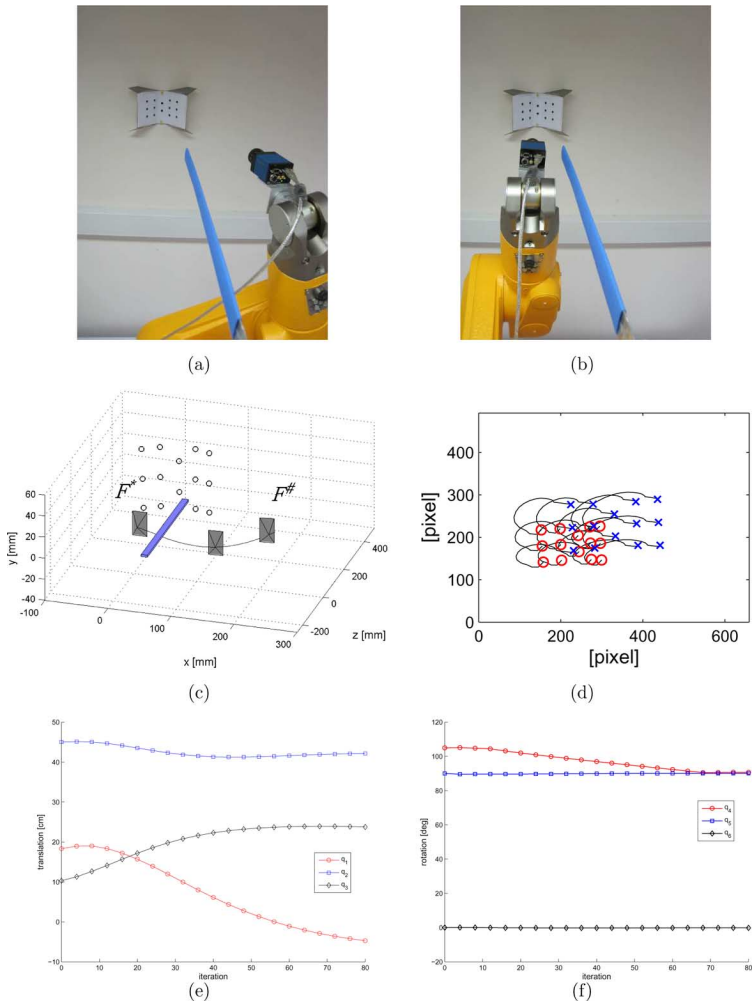

Fig. 4. Example 4. (a) Initial view. (b) Desired view. (c) 3D path. (d) Camera view ("O": initial view; "X": desired view). (e) Translation evolution. (f) Rotation evolution.

results, the constraint is fulfilled in spite of the present uncertainties.

C. Experimental Results: Example 3

Let us consider the experiment shown in Fig. 3. The problem consists of reaching the desired location avoiding collisions with an obstacle, which is represented by the blue bar in the initial and desired views shown in Fig. 3(a) and (b). The camera is roughly calibrated.

In order to show robustness of the proposed strategy against image noise and intrinsic calibration errors, we have placed the obstacle particularly close to one of the two extreme locations of the camera (specifically, the initial location). Observe in fact that uncertainties on the image points and intrinsic parameters unavoidably lead to errors on the estimated camera pose and, hence, on the estimated position of the obstacle with respect to the path of the camera. This fact is also explained by Fig. 1(b) which shows several desired locations produced by typical values of these uncertainties.

Hence, we introduce the family of admissible models $\mathcal{M}_1$ generated as in Example 1. We solve the robust path-planning problem (35) by modeling the obstacle as a box expanded in the z-direction in order to avoid that it could remain between the camera and the object points hence generating occlusions. Fig. 3(c)–(f) show the obtained results, in particular the 3-D path, the image trajectory and the evolution of the camera coordinates. As we can see, the camera successfully reaches the desired location avoiding collisions with and occlusions from the obstacle in spite of its vicinity to the initial location.

D. Experimental Results: Example 4

Fig. 4 considers another real experiment with a different configuration. Again the problem consists of reaching the desired location avoiding collisions with the obstacle. As in the experiment of Example 3, we have placed the obstacle particularly close to one of the two extreme locations of the camera (in this case, the desired location). This makes non-trivial for path-planning methods to fulfill the required constraints in the presence of image noise and intrinsic calibration errors.

VI. Conclusion

Path-planning is a useful strategy for visual servoing, however the planned reference trajectory is unavoidably affected by the presence of uncertainties on the used model. This paper has

proposed a new strategy for computing a robust reference trajectory, which consists of parametrizing a family of admissible reference trajectories via common design variables, and imposing the required constraints on all the parametrized reference trajectories.

ACKNOWLEDGMENT

The authors would like to thank the Editors and the Reviewers for their useful comments that have greatly improved this paper.

REFERENCES

[1] F. Chaumette and S. Hutchinson, "Visual servo control, part I: Basic approaches," *IEEE Robot. Autom. Mag.*, vol. 13, no. 4, pp. 82–90, Dec. 2006.

[2] F. Chaumette and S. Hutchinson, "Visual servo control, part II: Advanced approaches," *IEEE Robot. Autom. Mag.*, vol. 14, no. 1, pp. 109–118, Mar. 2007.

[3] , G. Chesi and K. Hashimoto, Eds., *Visual Servoing via Advanced Numerical Methods*. New York: Springer, 2010.

[4] Y. Mezouar and F. Chaumette, "Path planning for robust image-based control," *IEEE Trans. Robot. Autom.*, vol. 18, no. 4, pp. 534–549, 2002.

[5] L. Deng, F. Janabi-Sharifi, and W. J. Wilson, "Hybrid motion control and planning strategy for visual servoing," *IEEE Trans. Ind. Electron.*, vol. 52, no. 4, pp. 1024–1040, Jul./Aug. 2005.

[6] J. S. Park and M. J. Chung, "Path planning with uncalibrated stereo rig for image-based visual servoing under large pose discrepancy," *IEEE Trans. Robot. Autom.*, vol. 19, no. 2, pp. 250–258, Mar./Apr. 2003.

[7] Y. Mezouar and F. Chaumette, "Optimal camera trajectory with image-based control," *Int. J. Robot. Res.*, vol. 22, no. 10–11, pp. 781–803, 2003.

[8] V. Kyrki, D. Kragic, and H. I. Christensen, "New shortest-path approaches to visual servoing," in *Proc. Int. Conf. Intell. Robots Syst.*, 2004, pp. 349–354.

[9] B. Allotta and D. Fioravanti, "3D Motion planning for image-based visual servoing tasks," in *Proc. IEEE Int. Conf. Robot. Autom.*, 2005, pp. 2173–2178.

[10] G. Morel, P. Zanne, and F. Plestan, "Robust visual servoing: Bounding the task function tracking errors," *IEEE Trans. Control Syst. Technol.*, vol. 13, no. 6, pp. 998–1009, Nov. 2005.

[11] G. Chesi, "Visual servoing path-planning via homogeneous forms and LMI optimizations," *IEEE Trans. Robot.*, vol. 25, no. 2, pp. 281–291, Apr. 2009.

[12] M. Kazemi, K. Gupta, and M. Mehrandezh, "Global path planning for robust visual servoing in complex environments," in *Proc. IEEE Int. Conf. Robot. Autom.*, 2009, pp. 1726–1732.

[13] B. Espiau, "Effect of camera calibration errors on visual servoing in robotics," presented at the 3rd Int. Symp. Experimental Robot., Kyoto, Japan, 1993.

[14] V. Kyrki, D. Kragic, and H. Christensen, "Measurement errors in visual servoing," *Robot. Autonomous Syst.*, vol. 54, no. 10, pp. 815–827, 2006.

[15] G. Chesi, "Optimal object configurations for minimizing the positioning error in visual servoing," *IEEE Trans. Robot.*, vol. 26, no. 3, pp. 584–589, Jun. 2010.

[16] G. Chesi, "Designing image trajectories in the presence of uncertain data for robust visual servoing path-planning," in *Proc. IEEE Int. Conf. Robot. Autom.*, 2009, pp. 1492–1497.

[17] G. Chesi, "Camera displacement via constrained minimization of the algebraic error," *IEEE Trans. Pattern Anal. Mach. Intell.*, vol. 31, no. 2, pp. 370–375, Feb. 2009.

[18] G. Hu, N. Gans, N. Fitz-Coy, and W. Dixon, "Adaptive homography-based visual servo tracking control via a quaternion formulation," *IEEE Trans. Control Syst. Technol.*, vol. 18, no. 1, pp. 128–135, Jan. 2010.

[19] E. Malis and F. Chaumette, "2 1/2 D visual servoing with respect to unknown objects through a new estimation scheme of camera displacement," *Int. J. Computer Vision*, vol. 37, no. 1, pp. 79–97, 2000.

[20] G. Chesi and K. Hashimoto, "A simple technique for improving camera displacement estimation in eye-in-hand visual servoing," *IEEE Trans. Pattern Anal. Mach. Intell.*, vol. 26, no. 9, pp. 1239–1242, Sep. 2004.

[21] G. Chesi and Y. S. Hung, "Fast multiple-view L2 triangulation with occlusion handling," *Comput. Vision Image Understand.*, vol. 115, no. 2, pp. 211–223, 2011.

[22] G. Chesi, "LMI techniques for optimization over polynomials in control: A survey," *IEEE Trans. Autom. Control*, vol. 55, no. 11, pp. 2500–2510, Nov. 2010.

[23] H. Wang, Y.-H. Liu, and W. Chen, "Uncalibrated visual tracking control without visual velocity," *IEEE Trans. Control Syst. Technol.*, vol. 18, no. 6, pp. 1359–1370, Nov. 2010.

Graziano Chesi (SM'06) received the Laurea degree in information engineering from the University of Florence, Florence, Italy, in 1997 and the Ph.D. degree in systems engineering from the University of Bologna, Bologna, Italy, in 2001.

He was with the Department of Information Engineering, University of Siena, during 2000–2006 and then he joined the Department of Electrical and Electronic Engineering, University of Hong Kong. He is first author in more than 100 technical publications. He is author of the book *Homogeneous Polynomial Forms for Robustness Analysis of Uncertain Systems* (Springer, 2009), editor of the book *Visual Servoing via Advanced Numerical Methods* (Springer, 2010), and author of the book *Domain of Attraction: Analysis and Control via SOS Programming* (Springer, 2011).

Dr. Chesi has served as an Associate Editor for *Automatica*, *BMC Research Notes*, the *European Journal of Control*, the IEEE TRANSACTIONS ON AUTOMATIC CONTROL, and *Systems & Control Letters*. Also, he has served as Guest Editor of the Special Issues on Positive Polynomials in Control, Systems Biology, and Visual Servoing for various journals. He is the Founder and Chair of the Technical Committee on Systems with Uncertainty of the IEEE Control Systems Society.

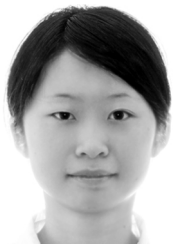

Tiantian Shen (S'10) received the B.S. degree in mechatronic engineering from China Agricultural University, Beijing, China, in 2006, and the M.S. degree in photogrammetry and remote sensing from Peking University, Beijing, China, in 2009. She is currently pursuing the Ph.D. degree in electrical and electronic engineering with the University of Hong Kong, Hong Kong.

Her current research interests include motion and structure estimation in computer vision and visual servoing in robotic control.